PET Imaging of Prostate Cancer Using Carbon-11-Choline

Toshihiko Hara, Noboru Kosaka and Hiroichi Kishi
Departments of Radiology and Urology, International Medical Center of Japan, Tokyo, Japan

Prostate cancer is difficult to visualize using current techniques. Recently, ^{31}P magnetic resonance spectroscopy has revealed that the tumor, in general, is characterized by an increased uptake of choline into the cell to meet increased synthesis of phosphatidylcholine, an important cell membrane phospholipid. We succeeded in using ^{11}C-choline to visualize prostate cancer and its local metastasis in PET. **Methods:** PET was performed on 10 prostate cancer patients from the level of pelvis to the lower abdomen. After transmission scanning, 370 MBq ^{11}C-choline were injected intravenously. The emission scan was performed 5–15 min postinjection. Finally, PET images were displayed so that each pixel was painted by a specified color representing the degree of the standardized uptake value (SUV). The ^{11}C-choline image was compared with the ^{18}F-fluorodeoxyglucose (FDG) image obtained from the same patient. **Results:** Imaging of prostate cancer and its local metastasis was difficult when ^{18}F-FDG was used because, within the pelvis, the areas of high uptake were concealed by the overwhelmingly abundant radioactivity in urine (in ureters and bladder). By contrast, it was easy when ^{11}C-choline was used because the urinary activity was negligible and tumor uptake was marked. The radioactivity concentration of ^{11}C-choline in prostate cancer and metastatic sites was at an SUV of more than three in most cases. The SUV of ^{18}F-FDG was considerably lower than that of ^{11}C-choline. **Conclusion:** Prostate cancer and its local metastasis were visualized clearly in PET using ^{11}C-choline.

Key Words: PET; carbon-11-choline; prostate cancer

J Nucl Med 1998; 39:990–995

Prostate cancer is a type of cancer in which it is difficult to determine the extent of its invasion and metastasis by current techniques. As a result, it also is difficult to estimate the outcome of surgery, radiotherapy, chemotherapy and hormonal therapy.

Despite the effectiveness of ^{18}F-fluorodeoxyglucose (FDG) PET in imaging various tumors, this technique is not appropriate for prostate cancer detection because the urinary excretion of ^{18}F-FDG is so large that it interferes with the imaging of tumors in the pelvis.

Recently, ^{31}P magnetic resonance spectroscopy (MRS) in vivo and in vitro has revealed an elevated level of phosphatidylcholine in tumors, which is the most abundant phospholipid in the cell membranes of all eukaryotic cells (*1–8*). It is thought that this elevation is the result of increased uptake of choline, a precursor of the biosynthesis of phosphatidylcholine (*9–14*).

We previously reported an application of ^{11}C-labeled choline for imaging brain tumors using PET (*15*). Since then, we successfully used this tracer to image many other types of tumors (*16*). Urinary excretion is negligible with ^{11}C-choline. Here we report the effectiveness of this tracer in PET imaging of prostate cancer in patients.

The tissue uptake of ^{11}C-choline is rapid after the intravenous injection, in accord with the rapid blood clearance (*15*). Once the radioactivity is absorbed into the tissue, the tissue uptake does not change for a long time with decay correction. It is practically constant from 5 to 40 min after injection in most organs. Because of these characteristics, the entire procedure of ^{11}C-choline PET in one patient takes 40 min.

MATERIALS AND METHODS

Patients

With our ethics committee's approval and the patients' informed consent, 10 patients who were admitted to the urology department of our hospital participated in this study. They had both ^{11}C-choline PET and ^{18}F-FDG PET studies before the beginning of treatment (two patients were reexamined after treatment, as discussed later). The PET studies were performed over 2 days before noon while patients were in the fasting state. Histological diagnosis was obtained on all patients before the PET study.

Radiopharmaceutical

Carbon-11-choline was prepared according to the method reported previously (*15*). Briefly, using a cyclotron to produce ^{11}C, and after reacting ^{11}C-methyl iodide with "neat" dimethylaminoethanol at 120°C for 5 min, the resulting product, ^{11}C-choline, was purified by evaporation of unreacted substrates followed by treatment of the remaining substance with cation-exchange resin (−COOH form), yielding an injection solution dissolved in saline. All synthetic and purification procedures were performed in an automated apparatus (Japan Steel Works, Muroran, Hokkaido, Japan).

Imaging Protocol

PET images were obtained using a PET camera (Headtome IV, 6-mm spatial resolution, Shimadzu, Kyoto, Japan) equipped with three rings to produce five slices at 13-mm intervals. For ^{11}C-choline, after acquiring transmission data, 370 MBq ^{11}C-choline were injected. Five minutes later, the emission scan was started. For ^{18}F-FDG, after acquiring transmission data followed by injection of 370 MBq ^{18}F-FDG, the patient was allowed to void. After placing the patient in the fixed bed position, the emission scan was started 40 min after injection. During transmission and emission scanning, the bed position was shifted six times upward from the level of pelvis to that of liver, with a total data acquisition time of 18 min. PET images were reconstructed after correcting the emission data by the transmission data. The horizontal images were displayed sequentially on a computer screen, where their slice levels were shown in a planar image made up from a whole set of the horizontal images (The planar image was helpful in determining the position of the prostate.) Finally, the horizontal images were displayed on the screen using a scale of the standardized uptake value (SUV). SUV is defined as:

$$SUV = \frac{\text{Regional radioactivity concentration}}{\text{Total injected dose/body weight}},$$

where the radioactivity concentration in a pixel (Bq/ml) was to be determined from an apparent pixel count (cps/pixel volume) and a

Received Feb. 1, 1997; revision accepted Oct. 9, 1997.
For correspondence or reprints contact: Toshihiko Hara, MD, Department of Radiology, International Medical Center of Japan, 1-21-1 Toyama, Shinjuku-ku, Tokyo 162, Japan.

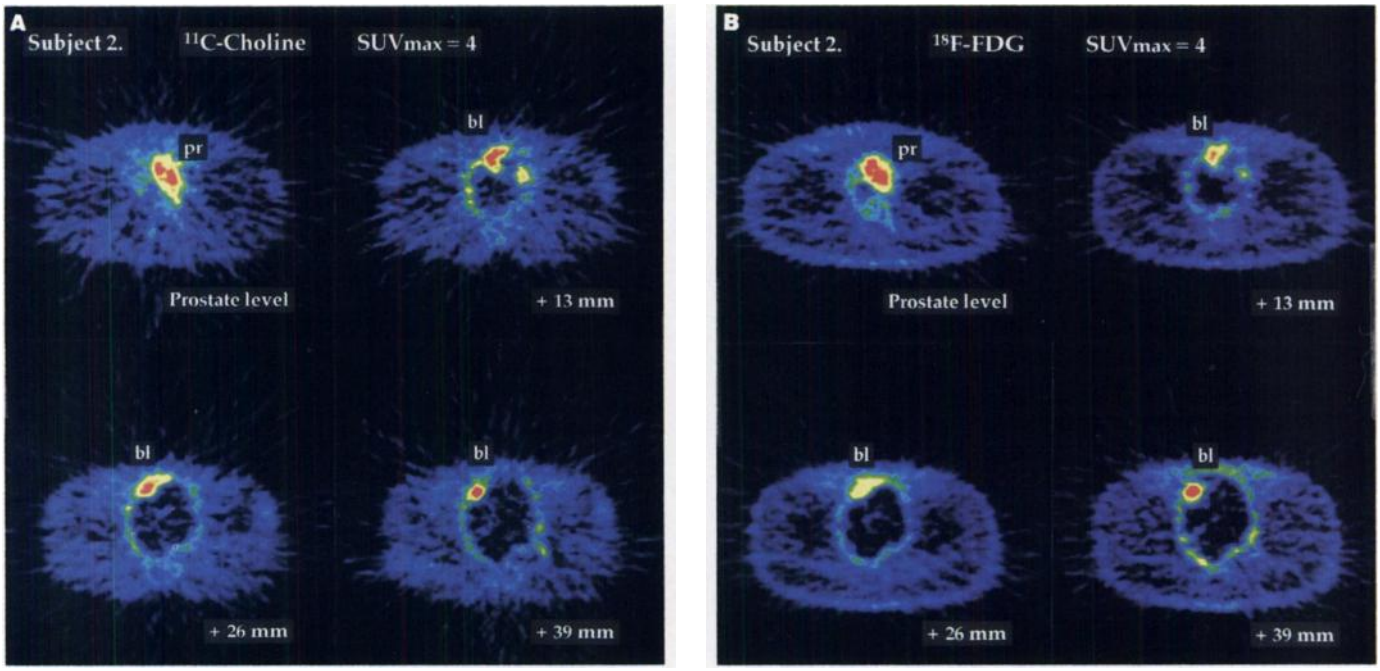

FIGURE 1. (A) Carbon-11-choline PET and (B) ^{18}F-FDG PET images of prostate cancer (Subject 2). Bilateral nephrostomy is inserted into the patient. The images are at the levels equal to and 13, 26 and 39 mm superior to the prostate level, respectively. They are displayed so that the pixel containing the highest uptake dose (SUV = 4.0 or more) is painted red. Pr = prostate; bl = urinary bladder.

predetermined cofactor. Each pixel (4 × 4 × 6 mm in real size) was painted a specified color that corresponded to the radioactivity concentration in it. Usually the red color (the brightest, hottest color) in the image was adjusted to an SUV of 4.0 or more. We called the image in which red was equal to an SUV of 4.0 "an image at SUV_{max} = 4." However, accurate calculation of SUV in a particular region of interest (ROI) was made using the ROI software in the PET computer from the average count of more than 20 pixels.

The most important patient variable was abstinence from food intake on the morning of the examination. If ^{11}C-choline PET was performed soon after food intake, the radioactivity incorporated into the pancreas came into pancreatic juice and then migrated into small intestines. The result was the appearance of an artifact in the image. Consequently, ^{11}C-choline PET always was performed before noon while the patient was in the fasting state. Nevertheless, sometimes we encountered radioactivity that seemed to have come from pancreatic juice, which usually looked like a string. The possible hazard of assuming this artifact to be true uptake was avoided by asking the patient to remain still at the end of scanning. We then looked at the PET image immediately. If there was any doubtful radioactivity in the image, we began the emission scan again. If pancreatic juice was involved, the second scan should have given a different image from the first. This procedure also was helpful in distinguishing urinary activity, if any, from true tissue uptake.

RESULTS

Carbon-11-Choline Uptake in the Normal Prostate

The prostate was the only organ in the pelvis that took up ^{11}C-choline significantly. The degree of uptake of ^{11}C-choline in the prostate, measured in four normal subjects (aged 54, 59, 62 and 66 yr), were SUVs of 1.86, 3.01, 3.28 and 2.83, respectively. The uptake in other organs in the pelvis was less than 1. The radioactivity in urine was negligible.

Case Presentation

Case 1. An 84-yr-old man (Fig. 1; Subject 2 in Table 1) was admitted to our hospital because of urinary retention and renal failure. Urethral catheterization was unsuccessful. Bilateral percutaneous nephrostomy was performed immediately afterward. A diagnosis of well-differentiated squamous cell carcinoma was made by transrectal needle biopsy of the prostate. CT revealed a large mass (8 cm in diameter) in the urinary bladder. Carbon-11-choline PET and ^{18}F-FDG PET were performed 1 wk later. With both tracers, high uptake was observed in the prostate and in the whole bladder wall, particularly in a mass localized in the anterior wall. The uptake in the prostate tumor as well as in the bladder mass was an SUV of about 4. SUVs in all other tissues within the pelvis were less than 1. Because of the bilateral nephrostomy performed on the patient, there was no radioactivity excreted into the bladder. The patient died 3 mo later from bacteremia, which was the result of vesicorectal penetration caused by invasion of the bladder cancer into the rectum. A partial autopsy was performed, and it indicated that the primary tumor was prostate cancer, of which the histological type confirmed the biopsy result as well-differentiated squamous cell carcinoma. The cancer invasion to the bladder and rectum was confirmed, but there was no metastasis to pelvic lymph nodes.

Case 2. A 72-yr-old man (Fig. 2; Subject 5 in Table 1) presented with urinary retention. The symptom was relieved by urethral catheterization. Transrectal needle biopsy of the prostate revealed poorly differentiated adenocarcinoma. On CT scans, the prostate was enlarged and slightly protruded into bladder. There was no enlargement of pelvic lymph nodes. Bone scintigraphy showed no abnormality in the pelvic bone. The prostate-specific antigen (PSA) level was 11.5. Both ^{11}C-choline PET and ^{18}F-FDG PET were performed. Carbon-11-choline PET showed a high uptake in the superior portion of the enlarged prostate and the bladder neck, each at an SUV of about 4. There also were small high-uptake areas in the right hip joint and coccyx. Fluorine-18-FDG PET provided almost no information about the disease state because the high level of radioactivity in urine obscured the pelvic structures (prostate cancer was discernible, however, when ^{11}C-choline PET image

TABLE 1
Uptake of Carbon-11-Choline and Fluorine-18-FDG in Pelvic Organs of a Normal Subject and Prostate Cancer Patients

Subject no.	Age (yr)	Prostate (determined by)	Local metastasis (determined by)	High-uptake areas with ^{11}C-choline other than prostate and local metastasis*	SUV†	
					^{11}C-choline	^{18}F-FDG
1	59	Normal prostate			3.01	2.92
				No		
2	84	Pr ca, sqm well (biopsy) (no uresis into bladder due to nephrostomy)			3.98	3.98
			Urinary bladder (CT)		3.79	3.88
				No		
3	80	Pr ca, adeno mod (biopsy)			3.27	1.74
			No			
				Spermatic cords	2.68	Invisible
4	75	Pr ca, adeno poor (biopsy)			4.33	3.29
			No			
				Pelvic lymph nodes, a few	6.46	2.77
5	72	Pr ca, adeno mod (biopsy) before prostatectomy			3.92	1.42
			Bladder neck (CT)		4.72	Urine
				Hip joint, right	1.91	1.13
				coccyx	1.75	1.04
		Same (second PET study), after prostatectomy			Prostate removed	
			Bladder neck (partial resection)		4.38	Urine
			Urethra (partial resection)		2.55	Invisible
			Hip joint, right (bone scan)		6.13	2.47
			Coccyx (bone scan)		2.47	1.20
6	70	Pr ca, adeno mod (biopsy)	No	No	4.59	1.91
7	69	Pr ca, adeno mod (biopsy)			4.76	1.70
			No			
				Pelvic lymph nodes, a few	3.98	1.90
8	68	Pr ca, adeno poor (biopsy), before hormonal therapy			2.91	1.65
			Ischia (bone scan, CT)		7.25	2.38
			Pubic bones (bone scan)		2.55	1.26
			Ilia (bone scan)		2.78	1.53
			Lumbar vertebra, L5 (bone scan, CT)		4.45	1.44
			Pelvic lymph nodes, multiple (CT)		3.68	1.67
				Acetabula	2.60	1.56
				Sacrum	2.58	1.51
		Same (second PET study), during hormonal therapy			2.90	2.07
			Ischia (bone scan, CT)		2.82	0.96
			Pubic bones (bone scan)		1.82	1.17
			Ilia (bone scan)		1.15	0.72
			Lumbar vertebra, L5 (bone scan, CT)		0.75	0.74
			Pelvic lymph nodes, multiple (CT)		3.21	1.40
			Intestinal wall (CT)		3.92	2.82
			Peritoneum (CT)		4.67	3.34
				Acetabula	2.81	Invisible
				Sacrum	1.34	1.26
				Coccyx	3.30	Invisible
				Bladder neck	3.74	Invisible
				Bladder	3.70	Urine
9	67	Pr ca, adeno well (biopsy)			3.47	1.62
			No			
				Pelvic lymph nodes, multiple	3.77	2.14
10	66	Pr ca, adeno mod (biopsy)			4.08	3.73
			No			
				Seminal vesicles	4.07	Urine
				Pelvic lymph nodes, multiple	3.69	4.99
11	62	Pr ca, adeno mod (biopsy)	No	No	3.64	2.11

*The high-uptake areas observable only with ^{18}F-FDG (i.e., ureters and bladder) are omitted from this table.

†The degree of uptake is indicated by standardized uptake value (SUV).

Pr ca = prostate cancer; sqm = squamous cell carcinoma; adeno = adenocarcinoma, well = well differentiated, mod = moderately differentiated; poor = poorly differentiated.

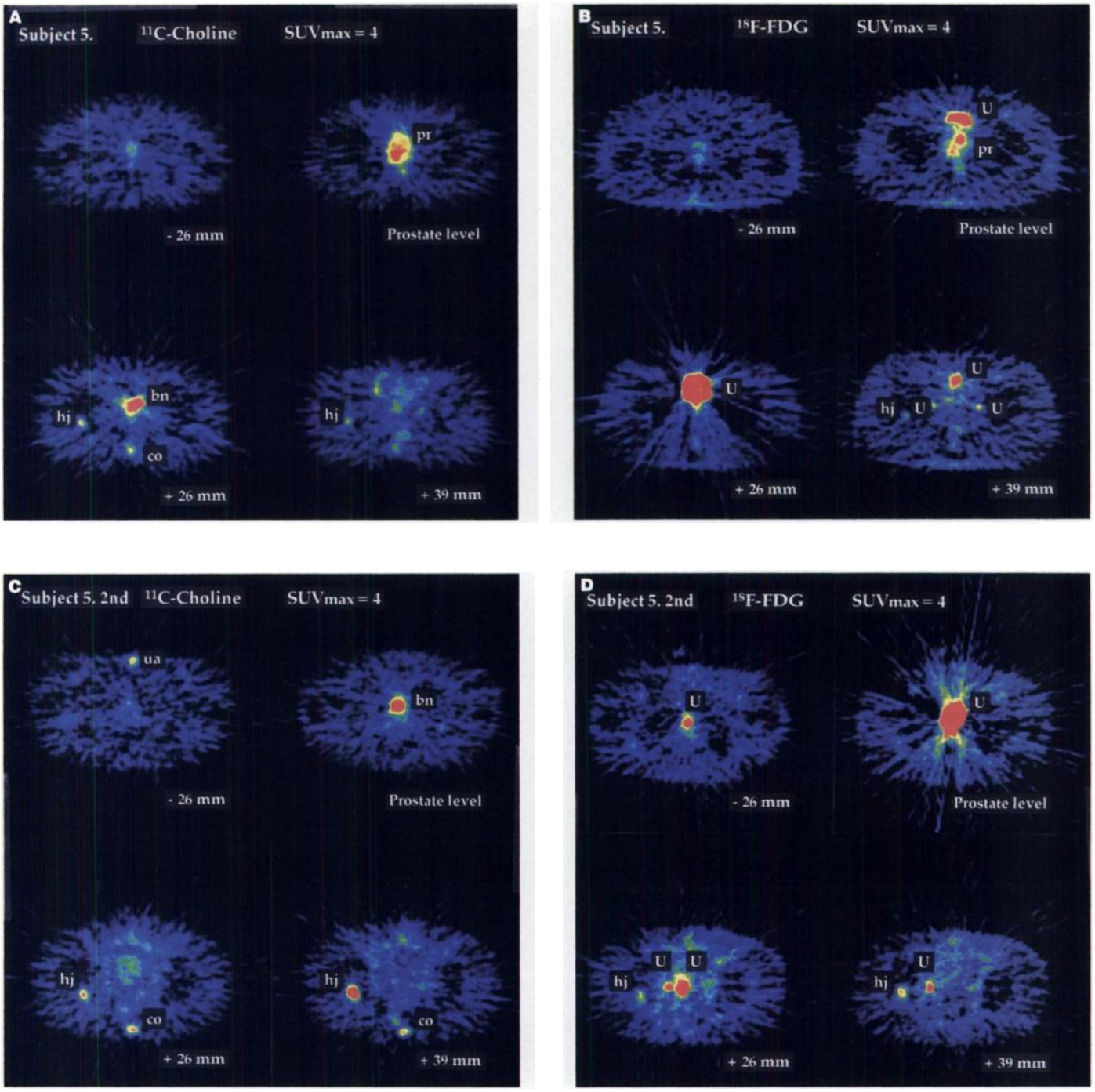

FIGURE 2. Carbon-11-choline and ^{18}F-FDG PET images of prostate cancer (Subject 5). Before prostatectomy: (A) ^{11}C-choline PET and (B) ^{18}F-FDG PET. After prostatectomy: (C) ^{11}C-choline PET and (D) ^{18}F-FDG PET. Bn = bladder neck; hj = hip joint; co = coccyx; U = urine; ua = urethra.

was used as a reference). Three months later, the patient had total prostatectomy, and a large area of tissue adjacent to the prostate was removed. Pathological examination of the removed tissue indicated that the tumor invasion was more advanced than was expected; it was invading the bladder neck and urethra. One month later, the PSA level was 8.2, but bone scintigraphy showed high uptake in the right hip joint and coccyx. Carbon-11-choline and ^{18}F-FDG PET were performed again. In the ^{11}C-choline PET image, there was a high uptake in the bladder neck (whose position was 26 mm below the previous one because of surgical defect), urethra, right hip joint and coccyx, which is consistent with the findings of other diagnostic means. Fluorine-18-FDG PET visualized an uptake in the right hip joint, albeit a small SUV.

Case 3. A 68-yr-old man (Fig. 3; Subject 8 in Table 1) was admitted to our hospital because of lumbago and edema in the left leg. The PSA level was 3054. Bone scintigraphy revealed high uptake in the lumbar vertebra, L5, as well as in the ischia, ilia and pubic bones. CT scans revealed the following abnormalities: osteolytic deformity in L5 and right ischium; enlargement of many pelvic lymph nodes (in the vicinity of aorta and common iliac and internal iliac arteries); and slight enlargement of the prostate bulging to the right posterior side. Transrectal needle biopsy of the prostate resulted in a diagnosis of poorly differentiated adenocarcinoma. Carbon-11-choline and ^{18}F-FDG PET were performed. Carbon-11-choline PET showed high uptake in all the abnormal sites and in the acetabula and sacrum. Fluorine-18-FDG PET provided information only

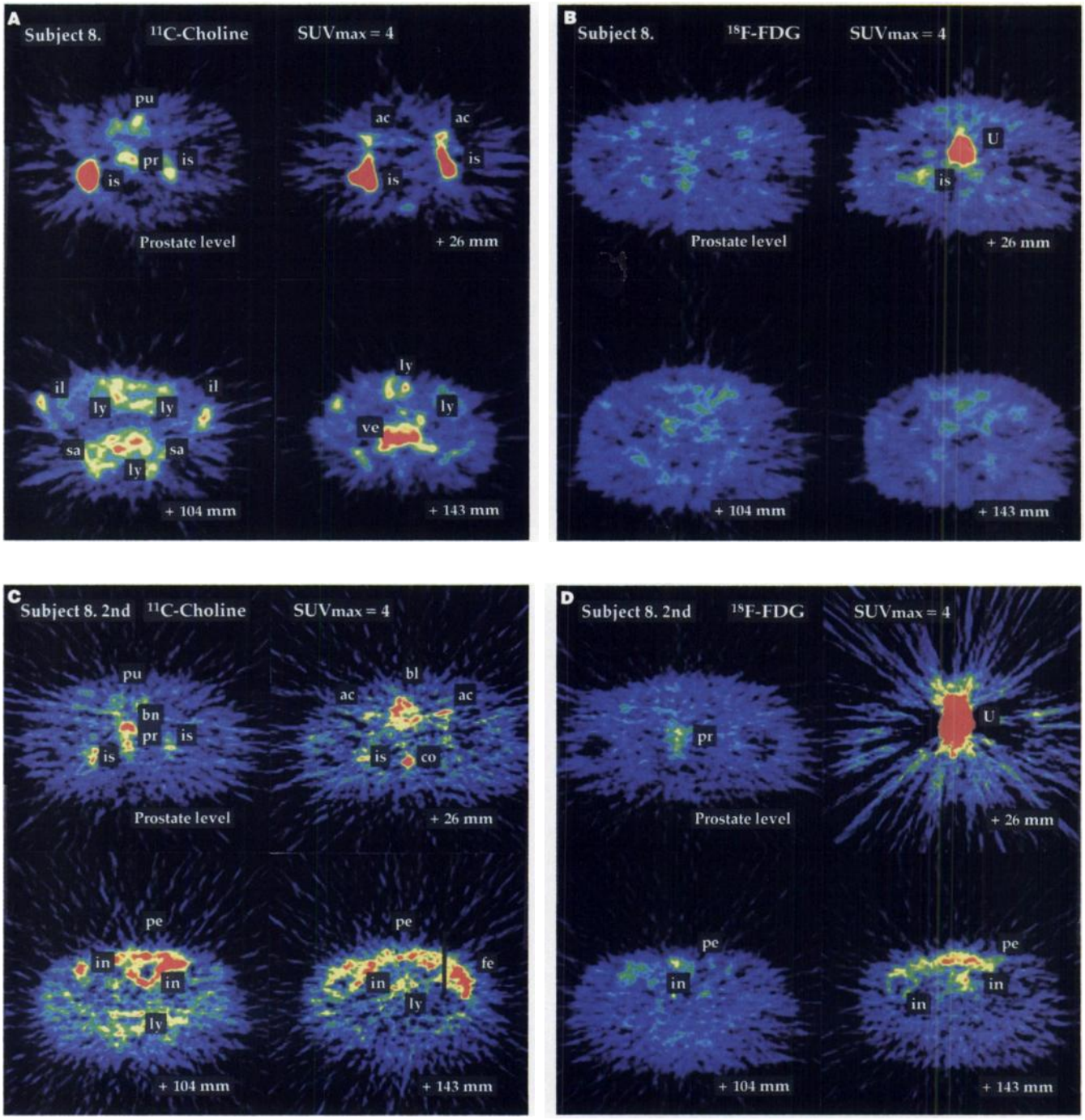

FIGURE 3. Carbon-11-choline and ^{18}F-FDG PET images of prostate cancer (Subject 8). Histology was poorly differentiated adenocarcinoma. Before hormonal therapy: (A) ^{11}C-choline PET and (B) ^{18}F-FDG PET. During hormonal therapy: (C) ^{11}C-choline PET and (D) ^{18}F-FDG PET. Is = ischium; pu = pubis; ac = acetabulum; il = ilium; sa = sacrum; ve = vertebra; ly = lymph node; in = intestinal wall; pe = peritoneum; fe = feces (pancreatic juice).

about radioactivity in the urine. Thereafter, the patient responded well to hormonal therapy, judging from the disappearance of lumbago and changes in PSA levels (173, 13.3 and 11.1 at 1, 2, and 3 mo later, respectively), but the left leg edema persisted. Carbon-11-choline and ^{18}F-FDG PET were performed again at the third month, and the findings were compared to CT and bone scintigraphy, which were taken soon after. The bone uptake of ^{11}C-choline, which was strikingly high previously, had diminished to the background level, and bone scintigraphy showed significantly reduced abnormality in bones. The prostate was smaller than previously depicted on CT scans. In spite of these favorable changes, several new abnormalities, suggestive of metastasis, were found. In ^{11}C-choline PET, there was high uptake in the intestinal wall, peritoneum, bladder neck, bladder wall and coccyx. In ^{18}F-FDG PET, there was high uptake in the intestinal wall and peritoneum. CT scans revealed multiple solid masses in the intestinal wall parenchyma, thickening of the peritoneum and adhesion of the intestinal wall with peritoneum.

Cumulated Results

The combined study of ^{11}C-choline and ^{18}F-FDG PET was performed on one normal subject and 10 prostate cancer patients, as shown in Table 1. The ^{11}C-choline uptake in both the normal prostate and prostate cancer was high, distinguishing them from other normal pelvic organs with low uptake. The

SUVs were almost the same between the normal prostate and prostate cancer. The ^{18}F-FDG uptake was considerably lower in those with prostate cancer (although the prostate image of ^{18}F-FDG was overshadowed by the large urine image of ^{18}F-FDG, they could be distinguished, more or less, because of the gap between them).

In ^{11}C-choline PET, uptake was high in primary prostate cancer, and this high uptake also was shared by the metastatic sites. The high uptake of ^{11}C-choline was found not only in already proved metastatic sites but also in other sites. These unidentified sites seemed to be small metastatic sites that could not be identified by other diagnostic means.

Carbon-11-choline PET was more sensitive than ordinary bone scintigraphy in detecting bone metastasis. This state of bone metastasis may be correctly called bone marrow metastasis. However, ^{18}F-FDG PET was not a sensitive diagnostic tool for detecting bone metastasis derived from prostate cancer.

DISCUSSION

New developments in imaging modalities and the general use of PSA have made the selection of options in treating prostate cancer easier than before and resulted in a preponderance of radical prostatectomy. Yet the method of determining intrapelvic metastasis is not accurate enough, and further developments are needed (*17*).

We introduced ^{11}C-choline PET as a new modality for imaging prostate cancer and its intrapelvic metastasis. The only pretreatment required of the patients was abstinence from food on the morning of the examination. This requirement was based on our observation in normal subjects. If ^{11}C-choline was injected soon after food intake, the radioactivity was secreted into pancreatic juice, which then appeared in the proximal portion of the small intestine. If ^{11}C-choline was injected in a fasting state, the radioactivity was retained in the pancreas and did not go into the small intestine. The radioactivity was absent in the gallbladder (bile), regardless of the prandial state. The radioactivity in pancreatic juice seemed to derive from the incorporation of ^{11}C-choline into phosphatidylcholine and its deacylated form, lysophosphatidylcholine, of pancreatic juice because it is known that it contains high concentrations of these compounds (*18*).

If there was radioactivity in the pelvis that was not accounted for, we traced the radioactivity from frame to frame in the serial image. If the dubious radioactivity accumulation was found only in one frame, it was likely that the radioactivity was from true tissue uptake, not from pancreatic juice.

Carbon-11-choline has a tendency to accumulate significantly in the liver, kidney (parenchyma) and spleen as well as the pancreas. Consequently, ^{11}C-choline PET could not be applied to tumor imaging in the upper abdomen. However, ^{11}C-choline PET was highly effective in imaging lung cancer and esophageal cancer localized in the chest (*16*).

The advantage of ^{11}C-choline PET over ^{18}F-FDG PET in the imaging of prostate cancer involved not only the absence of ^{11}C-choline activity in the urine but also the high uptake of ^{11}C-choline in the prostate cancer itself. The high uptake of choline in prostate cancer seems to be caused by two factors:

1. In general, tumor cells are characterized by the active incorporation of choline for production of phosphatidylcholine, a cell membrane constituent, to facilitate rapid cell duplication of tumor cells.
2. Normal cells of the prostate actively incorporate choline and produce phosphatidylcholine (*19*) and this property is found in prostate cancer cells.

By using three-dimensional ^{1}H MRS chemical shift imaging of the in situ human prostate, Kurhanewicz et al. (*20*) recently observed that the choline level in prostate cancer was significantly higher than in the normal prostate and benign prostatic hyperplasia. Because the choline signal in ^{1}H MRS originates from various types of choline-containing compounds and the intensity of the choline signal is influenced by their molecular environment (*21,22*), it remains to be determined which molecular species and what molecular condition are involved in this observation and how it is related to our observation.

CONCLUSION

By beginning PET scanning 5 min after injection of ^{11}C-choline, prostate cancer and its intrapelvic metastasis were visualized well in patients who had fasted on the morning of the examination.

ACKNOWLEDGMENTS

This work was supported in part by the Science and Technology Agency of Japan and the Japanese Smoking Research Foundation.

REFERENCES

1. Narayan P, Jajodia P, Kurhanewicz J, et al. Characterization of prostate cancer, benign prostatic hyperplasia and normal prostate using transrectal ^{31}P magnetic resonance spectroscopy: a preliminary report. *J Urol* 1991;146:66–74.
2. Narayan P, Kurhanewicz J. Magnetic resonance spectroscopy in prostate disease: diagnostic possibilities and future developments. *Prostate* 1992;4(suppl):43–50.
3. Daly PF, Cohen JS. Magnetic resonance spectroscopy of tumors and potential in vivo clinical applications: a review. *Cancer Res* 1989;49:770–779.
4. Shinkwin MA, Lenkinski RE, Daly JM, et al. Integrated magnetic resonance imaging and phosphorus spectroscopy of soft tissue tumors. *Cancer* 1991;67:1849–1858.
5. Negendank W. Studies of human tumors by MRS: a review. *NMR Biomed* 1992;5: 303–324.
6. Smith TAD, Bush C, Jameson C, et al. Phospholipid metabolites, prognosis and proliferation in human breast carcinoma. *NMR Biomed* 1993;6:318–323.
7. Merchant TE, van der Ven LTM, Minsky BD, et al. ^{31}P NMR phospholipid characterization of intracranial tumors. *Brain Res* 1994;649:1–6.
8. Aiken NR, Gillies RJ. Phosphomonoester metabolism as a function of cell proliferative status and exogenous precursors. *Anticancer Res* 1996;16:1393–1398.
9. Warden CH, Friedkin M. Regulation of choline kinase activity and phosphatidylcholine biosynthesis by mitogenic growth factors in 3T3 fibroblasts. *J Biol Chem* 1985;260:6006–6011.
10. Macara IG. Elevated phosphocholine concentration in *ras*-transformed NIH 3T3 cells arises from increased choline kinase activity, not from phosphatidylcholine breakdown. *Mol Cell Biol* 1989;9:325–328.
11. Teegarden D, Taparowsky EJ, Kent C. Altered phosphatidylcholine metabolism in C3H10T[1/2] cells transfected with the Harvey-*ras* oncogene. *J Biol Chem* 1990;265: 6042–6047.
12. Ronen SM, Rushkin E, Degani H. Lipid metabolism in T47D human breast cancer cells: ^{31}P and ^{13}C-NMR studies of choline and ethanolamine uptake. *Biochim Biophy Acta* 1991;1095:5–16.
13. Aiken NR, Szwergold ES, Kappler F, et al. Metabolism of phosphonium choline by rat-2 fibroblasts: effects of mitogenic stimulation studied using ^{31}P NMR spectroscopy. *Anticancer Res* 1996;16:1357–1364.
14. Katz-Brull R, Degani H. Kinetics of choline transport and phosphorylation in human breast cancer cells: NMR application of the zero trans method. *Anticancer Res* 1996;16:1375–1380.
15. Hara T, Kosaka N, Shinoura N, Kondo T. PET imaging of brain tumor with [*methyl*-^{11}C]choline. *J Nucl Med* 1997;38:842–847.
16. Hara T, Kosaka N, Kondo T, Kishi H, Kobori O. Imaging of brain tumor, lung cancer, esophagus cancer, colon cancer, prostate cancer, and bladder cancer with [^{11}C]choline [Abstract]. *J Nucl Med* 1997;38(suppl):250P.
17. Petrovich Z, Lieskovsky G, Luxton G, Baert L, Skinner DG. Adjuvant radiotherapy after radical prostatectomy in the management of carcinoma of the prostate. In: Petrovich Z, Baert L, Brady L, eds. *Carcinoma of the prostate: innovations in management*. Berlin: Springer-Verlag; 1996:283–301.
18. Vatier J, Poitevin C, Vitre MT, Mignon M. Caractérisation et évaluation du caractère pathogène du reflex duodénogastrique par la mesure de la choline et de l'acide sialique intragastriques chez le sujet normal et l'ulcéreux duodénal. *Gastroenterol Clin Biol* 1988;12:207–213.
19. Pulido JA, del Hoyo N, Pérez-Albarsanz MA. Composition and fatty acid content of rat ventral prostate phospholipids. *Biochim Biophys Acta* 1986;879:51–55.
20. Kurhanewicz J, Vigneron DB, Hricak H, Narayan P, Carroll P, Nelson SJ. Three-dimensional H-1 MR spectroscopic imaging of the in situ human prostate with high (0.24-0.7 cm^3) spatial resolution. *Radiology* 1996;198:795–805.
21. Miller BL. A review of chemical issues in ^{1}H NMR spectroscopy: N-acetyl-L-aspartate, creatinine and choline. *NMR Biomed* 1991;4:47–52.
22. Michaelis T, Merboldt KD, Bruhn H, Hänike W, Frahm J. Absolute concentrations of metabolites in the adult human brain in vivo: qualification of localized proton MR spectra. *Neuroradiology* 1993;187:219–227.